

Compressed Sensing and Parallel Acquisition

Il Yong Chun

Postdoctoral Research Associate
Department of Mathematics
Purdue University

Collaborators: Prof. Ben Adcock and Prof. Thomas M. Talavage

Communications & Signal Processing (CSP) Seminars
July 28th, 2016

†This work is partially supported by the Division of Mathematical Sciences of National Science Foundation (1318894) and Spinal Cord and Brain Injury Research Fund of the Indiana State Department of Health.

Work Experiences

- Intel Labs, Oregon, USA, 2011.
 - ▶ **“Real-time frequency-domain blind source separation of convolutive speech mixtures using non-stationarity in mobile environment”**
- Neuroscience Research Institute, Incheon, South Korea, 2013.
 - ▶ **“High-resolution PET image reconstruction with sparsity regularization and structural image”**
- Samsung Advanced Institute of Technology, Gyeonggi-do, South Korea, 2013.
 - ▶ **“Multi-modal image registration using double mutual information”**

Research Interests

- Ph.D. thesis in Purdue ECE ('15):
Advances in medical imaging and image reconstruction
- Practical compressed sensing (CS): Theory and application
 - ▶ I.Y. Chun and B. Adcock, "Compressed sensing and parallel acquisition," *submitted to IEEE Trans. Inf. Theory*, Jan. 2016, [Online] Available: <http://arxiv.org/abs/1601.06214>.
 - ▶ I.Y. Chun, B. Adcock, and T. Talavage, "Efficient compressed sensing SENSE pMRI with joint sparsity promotion," *IEEE Trans. Med. Imag.*, vol. 35, no. 1, pp. 354–368, Jan., 2016.
 - ▶ I.Y. Chun, B. Adcock, and T. Talavage, "Non-convex compressed sensing CT reconstruction based on tensor discrete Fourier slice theorem," in *Proc. IEEE EMBC*, Chicago, IL, Aug. 2014, pp. 5141–5144.
 - ▶ I.Y. Chun and T. Talavage, "Efficient compressed sensing statistical x-ray/CT reconstruction from fewer measurements," in *Proc. Intl. Mtg. on Fully 3D Image Recon. in Rad. and Nuc. Med.*, Lake Tahoe, CA, Jun. 2013, pp. 30–33.
- Adaptive signal processing in computational imaging
 - ▶ I.Y. Chun, S. Noh, D. Love, T. Talavage, S. Beckley, and S. Kisner "Mean squared error (MSE)-based excitation pattern design for parallel transmit and receive SENSE MRI image reconstruction," *IEEE Trans. Comput. Imag.* (under review), Jan., 2016.
- Statistical image analysis and its application in neuroimaging
 - ▶ I.Y. Chun, X. Mao, E. Breedlove, L. Leverenz, E. Nauman, and T. Talavage, "DTI detection of longitudinal WM abnormalities due to accumulated head impacts," *Dev. Neuropsychol.*, vol. 40, no. 2, pp. 92–97, May, 2015.
- Efficient algorithm derivation

Outline

1 CS and Parallel Acquisition

- Introduction
- Abstract Framework and Main Theorem
- Main Results: Distinct Sampling
- Main Results: Identical Sampling
- Numerical Experiments
- Conclusions

2 JS CS SENSE pMRI

- Introduction
- Theory & Methods
- Results & Discussion
- Conclusions

3 Future Research

4 Appx.

- CS and Parallel Acquisition
- JS CS SENSE pMRI

5 Appx.: CS X-Ray CT

Outline

1 CS and Parallel Acquisition

- Introduction
- Abstract Framework and Main Theorem
- Main Results: Distinct Sampling
- Main Results: Identical Sampling
- Numerical Experiments
- Conclusions

2 JS CS SENSE pMRI

- Introduction
- Theory & Methods
- Results & Discussion
- Conclusions

3 Future Research

4 Appx.

- CS and Parallel Acquisition
- JS CS SENSE pMRI

5 Appx.: CS X-Ray CT

Multiple Sensors in CS

Keywords

- Distributed CS
- Multiple measurement vector (MMV) model in CS
- Joint sparsity: Recovery of multiple signals with a shared support
- Best CS results: Exponential improvement in signal recovery failure probability with number of sensors (in MMV)

Environmental condition

- Communication channel between source signal \mathbf{x} and the sensors
- Geometric position of the sensors relative to \mathbf{x}
- Effectiveness of the sensors to \mathbf{x}
- Geometric features of the scene captured on sensors
- Can be widely modeled by structured matrices (e.g. diagonal, circulant, etc)

Can we achieve stronger CS results?

- To demonstrate benefits of multi-sensor over single-sensor architecture
- The average number of measurements required per sensor

$$m_{\text{avg}} \gtrsim C^{-1} s \times (\log \text{ factors}), \quad m_{\text{avg}} = C^{-1} \sum_{c=1}^C m_c,$$

decreases linearly in C as C increases, where C is the number of sensors.

System Model: CS and Parallel Acquisition

- System model: *Parallel acquisition*

$$\underbrace{\begin{bmatrix} \mathbf{y}_1 \\ \vdots \\ \mathbf{y}_C \end{bmatrix}}_{=:\mathbf{y}} = \underbrace{\begin{bmatrix} \mathbf{A}_1 \\ \vdots \\ \mathbf{A}_C \end{bmatrix}}_{=:\mathbf{A}} \mathbf{x} + \underbrace{\begin{bmatrix} \mathbf{e}_1 \\ \vdots \\ \mathbf{e}_C \end{bmatrix}}_{=:\mathbf{e}}$$

- ▶ $\mathbf{A}_c \in \mathbb{C}^{m_c \times N}$: measurement matrix in the c^{th} sensor; $\mathbf{e}_c \in \mathbb{C}^{m_c}$: noise; $m = \sum_c m_c$

- Recovery model: Quadratically-constrained basis pursuit

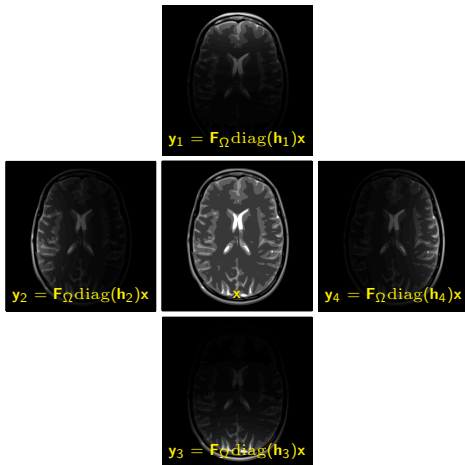
$$\min_{\mathbf{z} \in \mathbb{C}^N} \|\mathbf{z}\|_1 \text{ subject to } \|\mathbf{A}\mathbf{z} - \mathbf{y}\|_2 \leq \eta$$

- ▶ $\eta > 0$: $\|\mathbf{e}\|_2 \leq \eta$

- Identical sampling*: \mathbf{A}_c 's are dependent with $m_c = m/C$; $\mathbf{A}_c = \tilde{\mathbf{A}}\mathbf{H}_c$.
 - ▶ $\tilde{\mathbf{A}} \in \mathbb{C}^{m/C \times R}$: standard CS matrix (rand.); $\mathbf{H}_c \in \mathbb{C}^{R \times N}$: fixed & deterministic
- Distinct sampling*: \mathbf{A}_c 's are independent; $\mathbf{A}_c = \tilde{\mathbf{A}}_c\mathbf{H}_c$.
 - ▶ $\tilde{\mathbf{A}}_c \in \mathbb{C}^{m_c \times N_c}$; standard CS matrix (rand.); $\mathbf{H}_c \in \mathbb{C}^{N_c \times N}$: fixed & deterministic
- Sensor profile matrix* \mathbf{H}_c : Models environmental conditions; $\text{diag}(\mathbf{h}_c)$ & $\text{circ}(\mathbf{h}_c)$

Applications

- Parallel magnetic resonance imaging (pMRI)¹:
Identical Fourier sampling with $\text{diag}(\mathbf{h}_c)$ and C receive coils

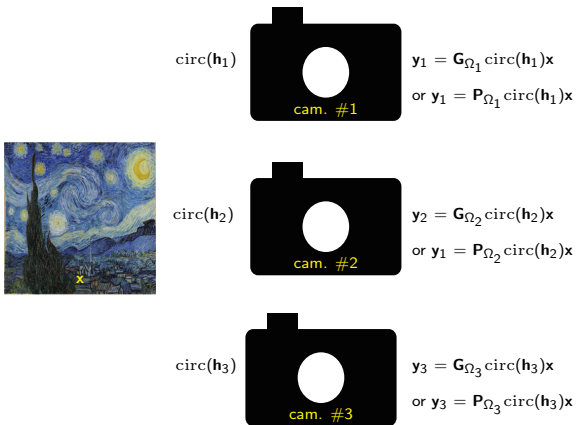


¹A worst-case bound (for noiseless case) is derived in I. Y. Chun, B. Adcock, and T. M. Talavage, "Efficient compressed sensing SENSE pMRI reconstruction with joint sparsity promotion", *IEEE Trans. Med. Imag.*, vol. 35, no. 1, pp. 354–368, 2016.

Applications

- Multi-view imaging²:

Distinct Gaussian (or binary) sampling³ with $\text{circ}(\mathbf{h}_c)$ and C cameras



²J. Y. Park and M. B. Wakin, "A geometric approach to multi-view compressive imaging", *EURASIP J. Adv. Signal Process.*, vol. 2012, no. 1, pp. 1–15, 2012.

³This requires a programmable sensing device, e.g. micromirror device.

Applications

- Papoulis' generalized sampling theorem⁴: Identical (C -fold downsampled) Fourier sampling with $\text{diag}(\mathbf{h}_c)$ and C linear functionals
- Other applications
 - ▶ System identification (observability problem): C observation times
 - ▶ Wireless sensor network: C wireless sensors
 - ▶ Light-field imaging: C focal lengths
- **CS benefits?** 1) scan time reduction, 2) recovery of higher dimensional or resolution signal, 3) power consumption reduction, etc.

⁴A. Papoulis, "Generalized sampling expansion", *IEEE Trans. Circuits Syst.*, vol. 24, no. 11, pp. 652–654, 1977.

Example: Multi-View Imaging⁵

1D distinct random convolution

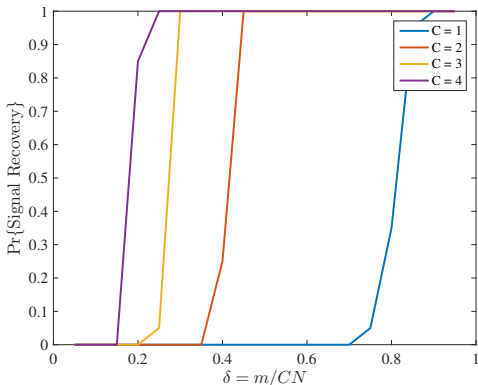


Figure: Empirical probability of successful sparse signal recovery in parallel random convolution sensing using distinct sampling with different number of sensors ($s = N/2$ and $C = 1, \dots, 4$): **This suggests that the number of measurements required per sensor can decrease as C increase.**

⁵Y. Traonmilin, S. Ladjal, and A. Almansa, "Robust multi-image processing with optimal sparse regularization", *J. Math. Imaging Vis.*, vol. 51, no. 3, pp. 413–429, 2015, M. F. Duarte and Y. C. Eldar, "Structured compressed sensing: From theory to applications", *IEEE Trans. Signal Process.*, vol. 59, no. 9, pp. 4053–4085, 2011

RIP vs RIPless

- The Restricted Isometry Property (RIP) is NP-hard to verify in general.
- The RIP often leads to a more stringent measurement condition (e.g. additional log factors).
 - ▶ **Uniform** recovery: A single random draw of \mathbf{A} guarantees recovery of **all** s -spares vectors, with high prob.
- **Nonuniform** recovery: A single random draw of \mathbf{A} guarantees recovery of **a fixed** s -sparse vector, with high prob.
e.g. RIPless theory by Candès & Plan⁶
 - ▶ The small exceptional set of matrices for which recovery fails may depend on the signal.
 - ▶ Better estimates both in terms of constants and asymptotic behavior than uniform recovery

⁶E. J. Candès and Y. Plan, "A probabilistic and RIPless theory of compressed sensing", *IEEE Trans. Inf. Theory*, vol. 57, no. 11, pp. 7235–7254, 2011.

Sparsity Models

Definition 1 (Sparsity)

A vector $\mathbf{z} \in \mathbb{C}^N$ is s -sparse for some $1 \leq s \leq N$ if $\|\mathbf{z}\|_0 \leq s$. We write Σ_s for the set of s -sparse vectors and, for an arbitrary $\mathbf{x} \in \mathbb{C}^N$, write

$$\sigma_s(\mathbf{x})_1 = \min \{ \|\mathbf{x} - \mathbf{z}\|_1 : \mathbf{z} \in \Sigma_s \},$$

for the error of the best ℓ^1 -norm approximation of \mathbf{x} by an s -sparse vector.

- In practice, vectors are not exactly s -sparse but *compressible* in the sense that they are well approximated by sparse ones. This is quantified by $\sigma_s(\mathbf{x})_p$, $p > 0$.
- $\mathbf{x} \in \mathbb{C}^N$ is *compressible* if $\sigma_s(\mathbf{x})_1$ is small, i.e. \mathbf{x} has s significant entries.
- Approximately s -sparse vector \mathbf{x} : We approximate \mathbf{x} by its largest s entries.

Beyond sparsity (Sparsity in levels⁷: new local principle)

- Sparsity is only a model based on a global principle.
- **Sparse and distributed signals** and **clustered sparse signals**⁷: sophisticated sparsity-in-levels models to better understand CS-based parallel acquisition system
- **Note: Claims related to sparsity in levels are omitted in this talk.**

⁷It is formally defined by Definition 3 in Appendix. See details in I. Y. Chun and B. Adcock, "Compressed sensing and parallel acquisition", *Submitted to IEEE Trans. Inf. Theory*, 2016. [Online]. Available: <http://arxiv.org/abs/1601.06214>.

Focus Today: A General Framework

- **Abstract framework** (a general framework)
 - ▶ Subgaussian random matrices, subsampled isometries, random convolutions ...
 - ▶ Distinct and identical sampling scenarios in parallel acquisition
- Generalization of *RIPlless* theory by Candès & Plan⁸ ($C = 1$)
- *Sparse and distributed* model: Based on *sparsity in levels* model⁹
- Improvement of results (e.g. log factors and error bound)
- An approximately sparse vector with support set Δ can be stably and robustly recovered from a number of noisy measurements

$$m \gtrsim D \cdot \Gamma(F, \Delta) \cdot L.$$

- ▶ D : a particular number dependent on the type of sampling ($D = 1$ or $D = C$)
- ▶ L : log term
- ▶ F : distribution from which the sensing matrix \mathbf{A} is drawn
- ▶ $\Gamma(F, \Delta)$: *local coherence of F relative to Δ*

⁸E. J. Candès and Y. Plan, "A probabilistic and RIPlless theory of compressed sensing", *IEEE Trans. Inf. Theory*, vol. 57, no. 11, pp. 7235–7254, 2011.

⁹B. Adcock, A. C. Hansen, C. Poon, *et al.*, "Breaking the coherence barrier: A new theory for compressed sensing", *ArXiv pre-print cs.IT/1302.0561*, 2013.

Focus Today: Sampling Scenarios

Distinct sampling ($\mathbf{H}_c = \mathbf{I}$)

- $\mathbf{A}_c \in \mathbb{C}^{m_c \times N}$'s are independently drawn from (possibly distinct) distributions F_c 's on \mathbb{C}^N .

Distinct sampling ($\mathbf{H}_c \neq \mathbf{I}$)

$$\mathbf{A}_c = \tilde{\mathbf{A}}_c \mathbf{H}_c$$

- $\tilde{\mathbf{A}}_c \in \mathbb{C}^{m_c \times N_c}$: standard CS matrix drawn from (possibly different) *isotropic* distribution G_c on \mathbb{C}^{N_c} .¹⁰
- $\mathbf{H}_c \in \mathbb{C}^{N_c \times N}$: fixed & deterministic sensor profile matrices

Identical sampling

$$\mathbf{A}_c = \tilde{\mathbf{A}} \mathbf{H}_c$$

- $\tilde{\mathbf{A}} \in \mathbb{C}^{m/C \times R}$: standard CS matrix drawn from *isotropic* distribution G on \mathbb{C}^R .¹¹
- $\mathbf{H}_c \in \mathbb{C}^{R \times N}$: fixed & deterministic sensor profile matrices

¹⁰ G_c 's are isotropic in the sense that $\mathbb{E}(\tilde{\mathbf{a}}_c \tilde{\mathbf{a}}_c^*) = \mathbf{I}$, $\tilde{\mathbf{a}}_c \sim G_c$.

¹¹ G is isotropic in the sense that $\mathbb{E}(\mathbf{a} \mathbf{a}^*) = \mathbf{I}$, $\mathbf{a} \sim G$

Background

- *RIPlless* CS¹²: $C = 1$ setting in our framework
- Construction of sensing matrix \mathbf{A} : Drawing m (col.) vectors i.i.d. from F ;

$$\mathbf{A} = \frac{1}{\sqrt{m}} \sum_{i=1}^m \mathbf{e}_i \mathbf{a}_i^*.$$

- ▶ F : distribution of vectors in \mathbb{C}^N
- ▶ $\{\mathbf{e}_i\}_{i=1}^m$: standard basis of \mathbb{C}^m
- *Isotropic* F : $\mathbb{E}(\mathbf{a}\mathbf{a}^*) = \mathbf{I}, \quad \mathbf{a} \sim F$
 - ▶ Components of $\mathbf{a} \sim F$ have unit variance and are uncorrelated.
 - ▶ With sufficient measurements, the sensing matrix is well conditioned, i.e. $m^{-1} \sum_{i=1}^m \mathbf{a}_i \mathbf{a}_i^* \approx \mathbf{I}$.
- *Coherence* of F : $\|\mathbf{a}\|_\infty^2 \leq \mu(F), \quad \mathbf{a} \sim F$
 - ▶ Sensing vectors with low coherence “spread out” information.
 - ▶ $\mathbb{E}|a_n|^2 = 1 \rightarrow \mu(F) \geq 1$
- s -sparse vector \mathbf{x} (i.e. $\|\mathbf{x}\|_0 \leq s$) can be recovered from the measurements $\mathbf{y} = \mathbf{A}\mathbf{x}$ using roughly $m \approx s \cdot \mu(F)$ measurements, up to log factors.

¹²E. J. Candes and Y. Plan, “A probabilistic and RIPlless theory of compressed sensing”, *IEEE Trans. Inf. Theory*, vol. 57, no. 11, pp. 7235–7254, 2011.

Abstract Framework: General Setup

- F : distribution on the space of $N \times D$ complex matrices, for some $D \in \mathbb{N}$.
- Construction of sensing matrix \mathbf{A} : Drawing p matrices i.i.d. from F ;

$$\mathbf{A} = \frac{1}{\sqrt{p}} \sum_{i=1}^p \mathbf{e}_i \otimes \mathbf{B}_i^* = \frac{1}{\sqrt{p}} \begin{bmatrix} \mathbf{B}_1^* \\ \vdots \\ \mathbf{B}_p^* \end{bmatrix} \in \mathbb{C}^{pD \times N}, \quad (1)$$

- ▶ F : distribution of matrices in $\mathbb{C}^{N \times D}$
- ▶ $\{\mathbf{e}_i\}_{i=1}^p$: standard basis of \mathbb{C}^p
- ▶ \otimes : Kronecker product

- Isotropic F :

$$\mathbb{E}(\mathbf{B}\mathbf{B}^*) = \mathbf{I}, \quad \mathbf{B} \sim F \quad (2)$$

- Both the distinct and identical sampling scenarios in parallel acquisition system can be represented by our general setup (see Appendix).

From Abstract Framework to Parallel Acq. System

| | RIPless setup | Abstract framework |
|-------|---|---|
| F | \mathbb{C}^N | $\mathbb{C}^{N \times D}$ |
| Cond. | F is isotropic: $\mathbb{E}(\mathbf{a}\mathbf{a}^*) = \mathbf{I}, \quad \mathbf{a} \sim F$ | F is isotropic: $\mathbb{E}(\mathbf{B}\mathbf{B}^*) = \mathbf{I}, \quad \mathbf{B} \sim F$ |

| | Distinct sampling | Identical sampling |
|-------|--|--|
| D | 1 | C |
| p | $m = \sum_{c=1}^C m_c$ | m/C |
| Cond. | F_c 's are joint. isotropic: $\sum_{c=1}^C \frac{m_c}{m} \mathbb{E}(\mathbf{a}_c \mathbf{a}_c^*) = \mathbf{I},$ $\mathbf{a}_c \sim F_c, c = 1, \dots, C$ | . |
| | Joint isometry for \mathbf{H}_c 's: $C^{-1} \sum_{c=1}^C \mathbf{H}_c^* \mathbf{H}_c = \mathbf{I}$ | Joint isometry for \mathbf{H}_c 's: $\sum_{c=1}^C \mathbf{H}_c^* \mathbf{H}_c = \mathbf{I}$ |

Table: Extension of isotropic conditions

Main Theorem

Theorem 2 (Abstract recovery guarantee¹³)

For $N, D, p \in \mathbb{N}$ with $N \geq 2$ and $pD \leq N$ let F be a distribution on $\mathbb{C}^{N \times D}$ satisfying (2) and suppose that $0 < \epsilon < 1$, $\eta \geq 0$ and $\Delta \subseteq \{1, \dots, N\}$ with $s = |\Delta| \geq 2$. Let $\mathbf{x} \in \mathbb{C}^N$ and draw $\mathbf{A} \in \mathbb{C}^{m \times N}$ according to (1), where $m = pD$. Then for any minimizer $\hat{\mathbf{x}}$ of

$$\min_{\mathbf{z} \in \mathbb{C}^N} \|\mathbf{z}\|_1 \text{ subject to } \|\mathbf{A}\mathbf{z} - \mathbf{y}\|_2 \leq \eta, \quad (3)$$

where $\mathbf{y} = \mathbf{A}\mathbf{x} + \mathbf{e}$ with $\|\mathbf{e}\|_2 \leq \eta$, we have

$$\|\mathbf{x} - \hat{\mathbf{x}}\|_2 \lesssim \|\mathbf{x} - \mathbf{P}_\Delta \mathbf{x}\|_1 + \sqrt{s}\eta, \quad (4)$$

with probability at least $1 - \epsilon$, provided¹⁴

$$m \gtrsim D \cdot \Gamma(F, \Delta) \cdot L,$$

where

$$L = \log(N/\epsilon) + \log(s) \log(s/\epsilon). \quad (5)$$

¹⁴The local coherence of F relative to Δ ($\Gamma(F, \Delta)$) is formally defined by Definition 4 in Appendix. It allows us to state our main results without defining a particular signal model, e.g. sparsity or sparsity in levels.

Main Results: Distinct Sampling

Recovery Guarantee: Dist. sampl. w/ sparsity model¹⁵

$$m \gtrsim s \cdot \left(\max_{c=1, \dots, C} \mu(F_c) \right) \cdot L$$

- ▶ F_c : distribution of \mathbf{A}_c ; $\mu(F_c)$: coherence of F_c , for $c = 1, \dots, C$
- ▶ F_1, \dots, F_C are **jointly isotropic**, i.e. $\sum_{c=1}^C \frac{m_c}{m} \mathbb{E}(\mathbf{a}_c \mathbf{a}_c^*) = \mathbf{I}$, $\mathbf{a}_c \sim F_c$.
- ▶ L is as in (5).

- Provided the sampling distributions are **incoherent** ($\mu(F_c) \approx 1 \forall c$) and **jointly isotropic**, we obtain an optimal recovery guarantee.

¹³I. Y. Chun and B. Adcock, "Compressed sensing and parallel acquisition", *Submitted to IEEE Trans. Inf. Theory*, 2016. [Online]. Available: <http://arxiv.org/abs/1601.06214>

¹⁵This is given by Corollary 6 in Appendix. See details in I. Y. Chun and B. Adcock, "Compressed sensing and parallel acquisition", *Submitted to IEEE Trans. Inf. Theory*, 2016. [Online]. Available: <http://arxiv.org/abs/1601.06214>

Main Results: Distinct Sampling

Recovery Guarantee: Dist. sampl. w/ sparsity model & diag. prof.¹⁶

$$m \gtrsim s \cdot \mu_G \cdot \left(\max_{c=1, \dots, C} \|\mathbf{H}_c\|_\infty^2 \right) \cdot L,$$

- ▶ $\mathbf{A}_c = \tilde{\mathbf{A}}_c \mathbf{H}_c$, $\mathbf{H}_c = \text{diag}(\mathbf{h}_c)$, for $c = 1, \dots, C$
- ▶ G_c : isotropic distribution of $\tilde{\mathbf{A}}_c$; $\mu(G_c)$: coherence of G_c , for $c = 1, \dots, C$
- ▶ $\mu_G = \max_{c=1, \dots, C} \mu(G_c)$
- ▶ \mathbf{H}_c 's satisfy the joint isometry condition $C^{-1} \sum_{c=1}^C \mathbf{H}_c^* \mathbf{H}_c = \mathbf{I}$.
- ▶ L is as in (5).

- Subject to incoherent sensing, one derives an optimal recovery guarantee provided $\|\mathbf{H}_c\|_\infty \lesssim 1$. Sensor profile design: one requires profiles which do not grow too large.

¹⁶This is given by Corollary 7 in Appendix. See details in I. Y. Chun and B. Adcock, "Compressed sensing and parallel acquisition", *Submitted to IEEE Trans. Inf. Theory*, 2016. [Online]. Available: <http://arxiv.org/abs/1601.06214>.

Summary of Results: Identical Sampling

- Our results for identical sampling are weaker than those for distinct sampling.
- A series of worst-case bounds (i.e. showing no improvement as C increases) are presented in Chun & Adcock¹⁷.
(These bounds are sharp in the sense that they are achieved by certain choices of the sensor profiles \mathbf{H}_C .)
- Within the **sparse and distributed model**, optimal recovery guarantees are possible by a general construction of sensor profile matrices. These sensor profile matrices are **diagonal** and have **piecewise constant blocks** (Theorem 4.7 in Chun & Adcock¹⁷).

¹⁷I. Y. Chun and B. Adcock, "Compressed sensing and parallel acquisition", *Submitted to IEEE Trans. Inf. Theory*, 2016. [Online]. Available: <http://arxiv.org/abs/1601.06214>.

Numerical Experiment (Phase Transition) Setup

• General setup

- ▶ For an s -sparse signal $\mathbf{x} \in \mathbb{C}^{128}$, s non-zero elements were chosen randomly and uniformly distributed on the unit circle.
- ▶ Phase transition graph of resolution 49×49
The horizontal and vertical axes are defined by $\delta = m/CN \in (0, 1)$ and $\kappa = s/N \in (0, 1)$ respectively.
- ▶ The empirical success fraction = $\#\{\text{successes}\}/20$ trials
Success corresponds to a relative recovery error $\|\mathbf{x} - \hat{\mathbf{x}}\|_2 / \|\mathbf{x}\|_2 < 0.001$.
- ▶ CVX's SDPT3¹⁸

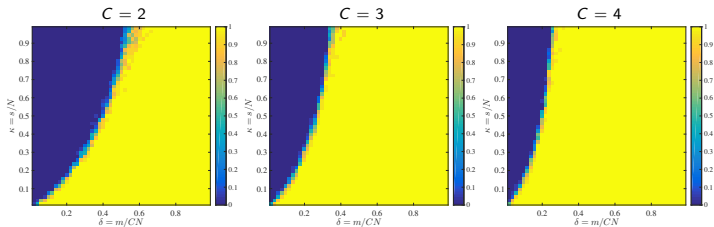
• Fourier sensing with complex diagonal sensor profile matrices¹⁹

- ▶ Its identical sampling scenario corresponds to a 1D example of the pMRI system model with *ideal* sensor profiles (i.e. satisfying the joint isometry cond.).
- ▶ Fourier sensing: m/C rows of the discrete Fourier transform (DFT) matrix were drawn uniformly at random without replacement
Distinct sampling: these rows were drawn independently across sensors.
- ▶ Sensor profile matrix: diagonal elements were generated using a truncated cosine function multiplied with phase vector $\{(c-1)2\pi/C + 2\pi/NC, \dots, c2\pi/C\}$.

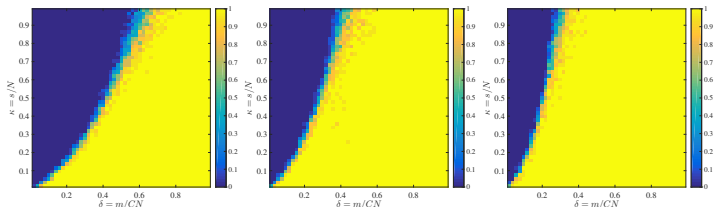
¹⁸I. CVX Research, *CVX: Matlab software for disciplined convex programming, version 2.0*, <http://cvxr.com/cvx>, 2012, M. Grant and S. Boyd, "Graph implementations for nonsmooth convex programs", in *Recent Advances in Learning and Control*, ser. Lecture Notes in Control and Information Sciences, 2008, pp. 95–110.

¹⁹The case of Gaussian sensing w/ circulant sensor profile matrices is omitted in this presentation. See its results in I. Y. Chun and B. Adcock, "Compressed sensing and parallel acquisition", *Submitted to IEEE Trans. Inf. Theory*, 2016. [Online]. Available: <http://arxiv.org/abs/1601.06214>.

Numerical Results: Fourier Sensing w/ Diagonal Profile Matrices



(a) Empirical phase transition for **distinct** sampling scenario



(b) Empirical phase transition for **identical** sampling scenarios

Figure: Empirical phase transitions for random Fourier sensing with diagonal sensor profile matrices and ($C = 2, 3, 4$) sensors (Chun & Adcock). For both sampling scenarios, the empirical probability of successful recovery increases as C increase.

Numerical Results:

Fourier Sensing w/ Diagonal Profile Matrices

- **Both the distinct and identical sampling scenarios:**

The empirical probability of successful recovery increases as the number of sensors C increases. The rate of increase is roughly linear in C .

- **Distinct sampling:**

The phase transition graphs confirm Corollary 7.

- **Identical sampling:**

Interestingly, even though the sensor profile matrices are not piecewise constant,²⁰ the phase transition curves show a similar increase.

→ Optimal recovery (i.e. linear decrease with C) is possible for identical sampling under broader conditions.

²⁰This is given by Theorem 4.7 in I. Y. Chun and B. Adcock, "Compressed sensing and parallel acquisition", *Submitted to IEEE Trans. Inf. Theory*, 2016. [Online]. Available: <http://arxiv.org/abs/1601.06214>.

Conclusions

- **Fundamental theoretical foundations to improve CS-based parallel acquisition systems in various applications**

Practical benefits: Cost, scan time, or power consumption reduction; resolution enhancement; higher dimensional signal reconstruction.

- **Our main theoretical results quantify the improvement:**

Recovery guarantees: The number of measurements required per sensor decreases linearly with the total number of sensors.²¹

- Specific case of diagonal or circulant sensor profile matrices in both the distinct and identical sampling scenarios:²¹

Our results give sufficient conditions for such optimal guarantees.

Such results are in agreement with the numerical experiments.

²¹I. Y. Chun and B. Adcock, "Compressed sensing and parallel acquisition", *Submitted to IEEE Trans. Inf. Theory*, 2016. [Online]. Available: <http://arxiv.org/abs/1601.06214>.

Outline

1 CS and Parallel Acquisition

- Introduction
- Abstract Framework and Main Theorem
- Main Results: Distinct Sampling
- Main Results: Identical Sampling
- Numerical Experiments
- Conclusions

2 JS CS SENSE pMRI

- Introduction
- Theory & Methods
- Results & Discussion
- Conclusions

3 Future Research

4 Appx.

- CS and Parallel Acquisition
- JS CS SENSE pMRI

5 Appx.: CS X-Ray CT

Introduction

Image Reconstruction in Parallel MRI (pMRI)

- Coil-by-coil image recon. (e.g. GRAPPA, SPIRiT, CaLM): Robustness to noise; inherently restricted to coil geometry, dependence of auto-calibration on sampl. trajectory
- Single image recon. (e.g. SENSE, CS SENSE, JSENSE, IRGN, Sparse BLIP): Optimal in recon. accuracy and imaging flexibility **if coil sensitivity estimation is accurate**; unguaranteed global solution in auto-calibration
- Third class (e.g. PRUNO, ESPIRiT, proposed JS CS SENSE²²): Benefits from both
- Calibration-less recon: Further imaging acceleration

Research Objective

- **Maximization of compressed sensing (CS) performance in pMRI**
 - ▶ **CS promoting joint sparsity (JS): Achievement of perfect image recovery with fewer measurements**
 - ▶ Efficient constrained JS ($\|\cdot\|_{2,1}$) minimization: Split Bregman (SB) & variable splitting (VS)
 - ▶ **Development of a theoretical foundation for CS-based medical imaging**
 - ▶ Calibration-less reconstruction framework

²²I. Y. Chun, B. Adcock, and T. M. Talavage, "Efficient compressed sensing SENSE pMRI reconstruction with joint sparsity promotion", *IEEE Trans. Med. Imag.*, vol. 35, no. 1, pp. 354–368, 2016, I. Y. Chun, B. Adcock, and T. Talavage, "Efficient compressed sensing SENSE parallel MRI reconstruction with joint sparsity promotion and mutual incoherence enhancement", in *Proc. 36th IEEE EMBS*, Chicago, IL, 2014, pp. 2424–2427.

Background

- Minimization problem for compressed sensing (CS)

$$\operatorname{argmin}_{\mathbf{x}} \|\Psi \mathbf{x}\|_1 \quad \text{s.t. } \mathbf{y} = \mathbf{P}_\Omega \Phi \mathbf{x},$$

- $\mathbf{x} \in \mathbb{C}^N, \mathbf{y} \in \mathbb{C}^N$
 - $\mathbf{P}_\Omega \in \mathbb{C}^{N \times N}$: select $\Omega \subseteq \{1, \dots, N\}, |\Omega| = m \ll N$ uniformly at random
 - $\Phi \in \mathbb{C}^{N \times N}$: orthonormal basis $\{\phi_n\}_{n=1}^N$, e.g. unitary DFT
 - $\Psi \in \mathbb{C}^{N \times N}$: orthonormal basis $\{\psi_n\}_{n=1}^N$, e.g. wavelet
- Perfect recovery of s -sparse solution in basis Ψ ($\|\Psi \mathbf{x}\|_0 := |\operatorname{supp}(\Psi \mathbf{x})| \leq s \ll N$) of $\mathbf{y} = \mathbf{P}_\Omega \Phi \mathbf{x}$ with high probability
- Recovery guarantee (sufficient measurement condition)

$$m \geq \kappa \mu(\mathbf{U})^2 N s \log N, \quad \text{for some constant } \kappa,$$

- Mutual coherence (MC) $\mu(\mathbf{U}) = \max_{i,j} |u_{i,j}| \in [1/\sqrt{N}, 1]$ & $\mathbf{U} = \Phi \Psi^{-123}$

²³E. J. Candes and Y. Plan, "A probabilistic and RIPless theory of compressed sensing", *IEEE Trans. Inf. Theory*, vol. 57, no. 11, pp. 7235–7254, 2011, B. Adcock and A. C. Hansen, "Generalized sampling and infinite-dimensional compressed sensing", *Found. Comput. Math.*, pp. 1–61, 2015.

System Model: pMRI

Discrete pMRI Model with SENSitivity Encoding (SENSE)²⁴

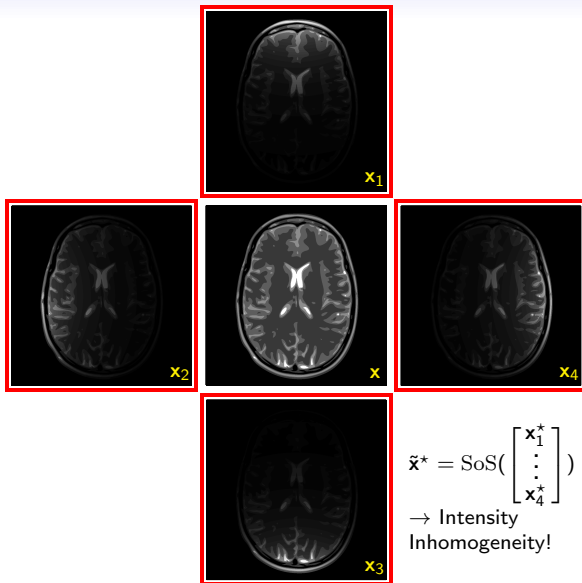
$$\underbrace{\begin{bmatrix} \mathbf{y}_1 \\ \vdots \\ \mathbf{y}_C \end{bmatrix}}_{=:\mathbf{y}} = \underbrace{\begin{bmatrix} \mathbf{P}_\Omega \Phi & & \\ & \ddots & \\ & & \mathbf{P}_\Omega \Phi \end{bmatrix}}_{=:\mathbf{F}_{\tilde{\Omega}}} \underbrace{\begin{bmatrix} \text{diag}(\mathbf{h}_1) \\ \vdots \\ \text{diag}(\mathbf{h}_C) \end{bmatrix}}_{=:\mathbf{H}} \mathbf{x} + \underbrace{\begin{bmatrix} \mathbf{n}_1 \\ \vdots \\ \mathbf{n}_C \end{bmatrix}}_{=:\mathbf{n}}$$

- ▶ $\mathbf{x} \in \mathbb{C}^N$, $\mathbf{y} \in \mathbb{C}^{NC}$, $\mathbf{n} \in \mathbb{C}^{NC}$, in which $\mathbf{n}_{c,\Omega} \sim \mathcal{CN}(0, \sigma_c \mathbf{I})$ for $c = 1, \dots, C$ ²⁵
- ▶ $\mathbf{F}_{\tilde{\Omega}} = \mathbf{P}_{\tilde{\Omega}} (\mathbf{I}_C \otimes \Phi) \in \mathbb{C}^{NC \times NC}$,
 in which $\Phi \in \mathbb{C}^{N \times N}$: 2D discrete Fourier transform (DFT),
 $\mathbf{P}_{\tilde{\Omega}} = (\mathbf{I}_C \otimes \mathbf{P}_\Omega) \in \mathbb{C}^{NC \times NC}$
 $|\tilde{\Omega}| = m$: $m = \sum_{c=1}^C m_c$ and $m_c = |\Omega| \ll N$
- ▶ $\mathbf{H} \in \mathbb{C}^{NC \times N}$,
 in which $\mathbf{h}_c \in \mathbb{C}^N$: receive sensitivity for the c^{th} coil for $c = 1, \dots, C$,
 $\text{diag}(\cdot)$: vector \Leftrightarrow diagonal matrix

²⁴K. P. Pruessmann, M. Weiger, M. B. Scheidegger, et al., "Sense: Sensitivity encoding for fast MRI", *Magn. Reson. Med.*, vol. 42, no. 5, pp. 952–962, 1999.

²⁵A. Macovski, "Noise in MRI", *Magn. Reson. Med.*, vol. 36, no. 3, pp. 494–497, 1996.

Coil-by-Coil Image Reconstruction



Coil-by-Coil Image Reconstruction

Minimization Problem (Coil-by-coil CS pMRI recon.²⁶)

Considering separability of opt. prob., an appl. of CS is straightforward:

$$\underset{\mathbf{x}_c}{\operatorname{argmin}} \underbrace{\|\Psi_c \mathbf{x}_c\|_1}_{\text{Sparsity of mult. coil imgs}} \quad \text{s.t.} \quad \underbrace{\|\mathbf{y} - \mathbf{F}_{\tilde{\Omega}} \mathbf{x}_c\|_2^2}_{\text{Data fidelity w/o SENSE}} < \delta.$$

- ▶ $\mathbf{x}_c = [x_1^* | \dots | x_c^*]^* \in \mathbb{C}^{NC}$,
in which $x_c \in \mathbb{C}^N$: unknown image for c^{th} coil for $c = 1, \dots, C$
- ▶ $\Psi_c = \mathbf{I}_C \otimes \Psi \in \mathbb{C}^{NC \times NC}$,
in which $\Psi \in \mathbb{C}^{N \times N}$: discrete Daubechies transform (DDT)
- Problem: 1) **Intensity inhomogeneity** and 2) phase information removal from sum-of-square (SoS) combination
 - ▶ SoS process for recon. of $\tilde{\mathbf{x}}$: $\tilde{x}_n = \sqrt{\sum_{c=1}^C |x_{c,n}|^2}$ for $n = 1, \dots, N$

²⁶A. Majumdar and R. K. Ward, "Calibration-less multi-coil MR image reconstruction", *Magn. Reson. Imaging*, vol. 30, no. 7, pp. 1032–1045, 2012, M. Murphy, M. Alley, J. Demmel, et al., "Fast l_1 -SPIRiT compressed sensing parallel imaging MRI: Scalable parallel implementation and clinically feasible runtime", *IEEE Trans. Med. Imag.*, vol. 31, no. 6, pp. 1250–1262, 2012

Coil-by-Coil CS pMRI Reconstruction

Recovery Guarantee (Coil-by-coil CS recon.)

$$m \gtrsim \eta \sum_c s_c \log N \xrightarrow[\text{Acq.}]{\text{Simul.}} m \gtrsim \eta C \left(\max_c s_c \right) \log(N)$$

▶ $s_c = \|\Psi \mathbf{x}_c\|_0$ for $c = 1, \dots, C$

- Linear in C and $\max_c s_c$
- Asymptotic MC²⁷

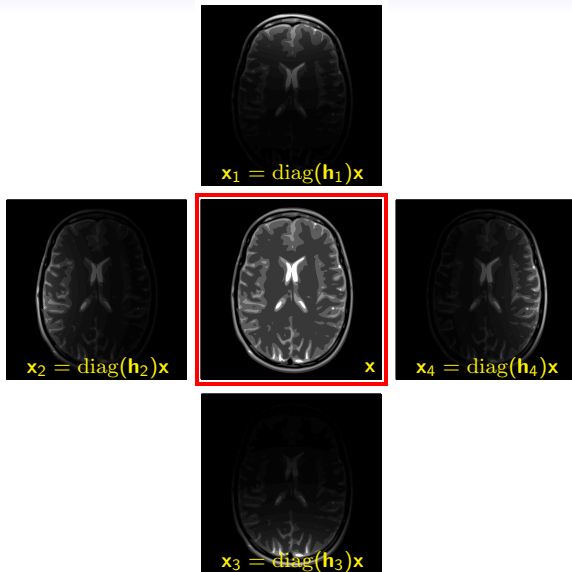
Remark (Asymptotic MC)

- $\mu(\Phi\Psi^*)^2 = \mathcal{O}(1)$ in practice
- Replacement of it with asymptotic MC using nonuniform sampl. $\rightarrow \mu(\Phi\Psi^*) \approx \sqrt{\eta/N}$ ²⁷
- **Radial line sampling**: Sufficiently close to the optimal nonuniform sampl. (see Appendix)²⁸

²⁷B. Adcock, A. C. Hansen, C. Poon, *et al.*, "Breaking the coherence barrier: A new theory for compressed sensing", *ArXiv pre-print cs.IT/1302.0561*, 2013

²⁸I. Y. Chun, B. Adcock, and T. Talavage, "Efficient compressed sensing SENSE parallel MRI reconstruction with joint sparsity promotion and mutual incoherence enhancement", in *Proc. 36th IEEE EMBS, Chicago, IL, 2014*, pp. 2424–2427

Single Image Reconstruction based on SENSE



CS SENSE pMRI Reconstruction

Problem (CS SENSE pMRI recon.²⁹)

Conventional CS SENSE pMRI reconstruction model:

$$\underset{\mathbf{x}}{\operatorname{argmin}} \underbrace{\|\Psi\mathbf{x}\|_1}_{\text{Sparsity of single img}} \quad \text{s.t.} \quad \underbrace{\|\mathbf{y} - \mathbf{F}_{\tilde{\Omega}}\mathbf{H}\mathbf{x}\|_2^2}_{\text{SENSE-based data fidelity}} < \delta.$$

- ▶ $\mathbf{x} \in \mathbb{C}^N$: unknown target image
- SENSE-based single image recon.:
Optimal and most flexible (in particular for coil geometry)!
- Performance bottleneck: **Estimation accuracy of \mathbf{H}**

²⁹I. Y. Chun, B. Adcock, and T. M. Talavage, "Efficient compressed sensing SENSE pMRI reconstruction with joint sparsity promotion", *IEEE Trans. Med. Imag.*, vol. 35, no. 1, pp. 354–368, 2016, H. She, R. R. Chen, D. Liang, et al., "Sparse BLIP: BLind Iterative Parallel imaging reconstruction using compressed sensing", *Magn. Reson. Med.*, vol. 71, no. 2, pp. 645–660, 2014

Recovery Guarantee (CS SENSE recon.³⁰)

$$m \gtrsim \eta Cs \log N$$

▶ $s = \|\Psi \mathbf{x}\|_0$

- Linear in C and s

- Simplifying assumptions

- ▶ $\Psi = \mathbf{I}$: Avoidance of MC barrier (i.e. high MC b/w Fourier and wavelet systems)³¹
- ▶ $\sum_c |\text{diag}(\mathbf{h}_c)|^2 = \mathbf{I}$: Prevention of the inhomogeneity problem (i.e. location-dependent bias problem in the resultant SoS-combined image)³²

- W/o the assumptions, slightly worse recovery guarantee in practice

³⁰This is given by Theorem 8 in Appendix. See details in I. Y. Chun, B. Adcock, and T. M. Talavage, "Efficient compressed sensing SENSE pMRI reconstruction with joint sparsity promotion", *IEEE Trans. Med. Imag.*, vol. 35, no. 1, pp. 354–368, 2016.

³¹B. Adcock, A. C. Hansen, C. Poon, *et al.*, "Breaking the coherence barrier: A new theory for compressed sensing", *ArXiv pre-print cs.IT/1302.0561*, 2013

³²E. G. Larsson, D. Erdogmus, R. Yan, *et al.*, "SNR-optimality of sum-of-squares reconstruction for phased-array magnetic resonance imaging", *J. Magn. Reson.*, vol. 163, no. 1, pp. 121–123, 2003

JS CS SENSE pMRI Reconstruction

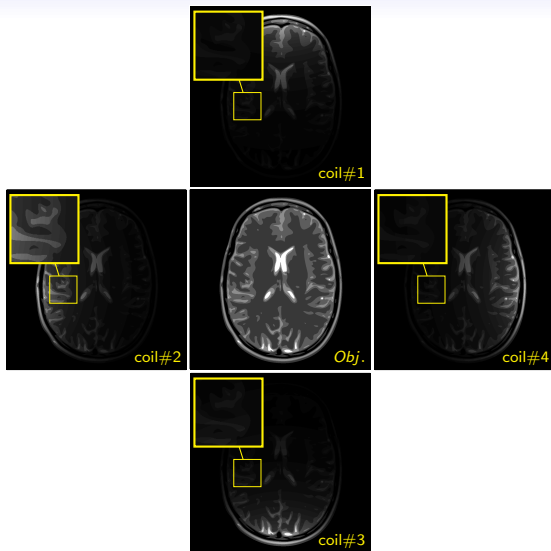


Figure: Sparsity across channels: shared sparsity pattern

JS CS SENSE pMRI Reconstruction

Problem (JS CS SENSE recon.³³)

Fully exploiting the relationship b/w the imgs in each coil, i.e. their **shared sparsity patterns**, the proposed joint sparsity (JS) CS SENSE is given by:

$$\underset{\mathbf{x}}{\operatorname{argmin}} \overbrace{\|\Psi_C \mathbf{H} \mathbf{x}\|_{2,1}}^{\text{JS of synthesized mult. coil imgs}} \quad \text{s.t.} \quad \underbrace{\|\mathbf{y} - \mathbf{F}_{\tilde{\Omega}} \mathbf{H} \mathbf{x}\|_2^2}_{\text{SENSE-based data fidelity}} < \delta. \quad (6)$$

- ▶ JS ($\|\cdot\|_{2,1}$): $\|\boldsymbol{\psi}\|_{2,1} = \sum_{n=1}^N \sqrt{\sum_{c=1}^C |\psi_{nc}|^2}$ (convex-functional)³⁴
- **SENSE-based single image recon.:** Avoidance of inhomogeneity artifacts
- Assumptions: $\bigcap_c \operatorname{supp}(\mathbf{h}_c) \neq \emptyset$ on Δ & smooth spatial profiles \mathbf{h}_c 's

³³I. Y. Chun, B. Adcock, and T. M. Talavage, "Efficient compressed sensing SENSE pMRI reconstruction with joint sparsity promotion", *IEEE Trans. Med. Imag.*, vol. 35, no. 1, pp. 354–368, 2016, I. Y. Chun, B. Adcock, and T. Talavage, "Efficient compressed sensing SENSE parallel MRI reconstruction with joint sparsity promotion and mutual incoherence enhancement", in *Proc. 36th IEEE EMBS*, Chicago, IL, 2014, pp. 2424–2427

³⁴P. Boufounos, G. Kutyniok, and H. Rauhut, "Sparse recovery from combined fusion frame measurements", *IEEE Trans. Inf. Theory*, vol. 57, no. 6, pp. 3864–3876, 2011

JS CS SENSE pMRI Reconstruction

“Worst case” recovery guarantee (JS CS SENSE recon.³⁵)

$$m \gtrsim \eta \sum_{c=1}^C s_c \log N \xrightarrow[\text{Acq.}]{\text{Simul.}} m \gtrsim \eta C \left(\max_{c=1, \dots, C} s_c \right) \log(N)$$

The analysis is based on the relaxed minimization of JS CS SENSE, i.e. coil-by-coil recon.

Note (Performance expectation)

- Dependence on size of support of sensitivities
- Dependence on imaging resolution
 Low resolution: $s_c \approx s/C$
 High resolution: $s_c \approx s$
- JS CS SENSE vs CS SENSE: $\sum_c s_c$ (or $\max_c s_c$) vs sC ;
 Greater difference in low-resolution imaging (see Appendix)

³⁵I. Y. Chun, B. Adcock, and T. M. Talavage, “Efficient compressed sensing SENSE pMRI reconstruction with joint sparsity promotion”, *IEEE Trans. Med. Imag.*, vol. 35, no. 1, pp. 354–368, 2016

Simulation Setup I

- Tested image: GLPU-phantom with size of 256×256 & 1024×1024 ³⁶;
 T_1 -weighted brain image with size of 512×512 (non-piecewise constant)
- The rectangular field-of-view (FOV) of size 25.6×25.6 cm
- Sensitivity map simulation (Biot-Savart law): $C = 2$, $C = 4$; a coil radius of 6 cm; a distance from the coil centers to the center of the rectangular FOV of 15 cm
- Sampling information for different images:

| 256 × 256 Phantom Radial line (# of lines) | | | 1024 × 1024 Phantom Radial line (# of lines) | | | 512 × 512 Human Brain Radial line (# of lines) | | |
|---|----------|----------|---|---------|----------|---|----------|----------|
| 36 | 48 | 62 | 47 | 70 | 95 | 47 | 59 | 71 |
| ≈ 15.0 % | ≈ 20.0 % | ≈ 25.0 % | ≈ 5.0 % | ≈ 7.5 % | ≈ 10.0 % | ≈ 10.0 % | ≈ 12.5 % | ≈ 15.0 % |

- Realization of complex Gaussian noise: relatively low noise (35 dB SNR) for phantom & low noise (40 dB SNR) for neuroimage (SNR: signal-to-noise ratio)
- Recon. parameters: SB suggestions³⁷; 4-level DDT of filter size 4 (DDT-4); $n_{Inner} \times n_{Outer}$ iteration is 1×10000 for GLPU phantom & 1×12500 for real T_1 -weighted image
- Recon. accuracy evaluation: $SER_{dB}(k) = 20 \log_{10}(\|\mathbf{x}^{true}\|_2 / \|\mathbf{x}^{true} - \mathbf{x}^{(k)}\|_2)$

³⁶M. Guerquin-Kern, L. Lejeune, K. P. Pruessmann, *et al.*, "Realistic analytical phantoms for parallel Magnetic Resonance Imaging", *IEEE Trans. Med. Imag.*, vol. 31, no. 3, pp. 626–636, 2012.

³⁷T. Goldstein and S. Osher, "The split Bregman method for L1-regularized problems", *SIAM J. Imaging Sci.*, vol. 2, no. 2, pp. 323–343, 2009.

Results: JS CS SENSE vs CS SENSE Recon.

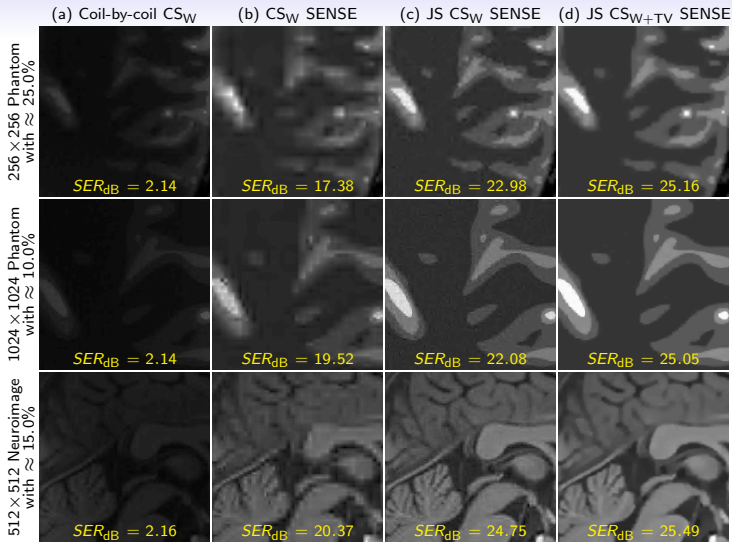


Figure: Comparison of reconstructed images from different CS pMRI reconstruction models and images (noisy measurements, convex models, and $C = 4$): SER gaps between (b) and (c) are [3.1, 7.2] dB for the 256×256 GLPU phantom, [1.5, 4.7] dB for the 1024×1024 GLPU phantom, and [3.5, 6.2] dB for the 512×512 neuroimage.

Conclusions

An Advantage of JS CS SENSE over CS SENSE

- More accurate reconstruction (e.g. up to 6.2 dB in SER for 512×512 neuroimage)
- @ Higher resolution imaging, less significant improvement in the recovery guarantee for JS CS SENSE over CS SENSE: e.g. $\sum_c s_c / C_s$ is 0.57 for 256×256 and 0.93 for 1024×1024 .

Advantages of Calibration-Less (CaL) JS CS SENSE over State-of-the-Art Methods

- More accurate reconstruction for complex and small-sized anatomical structures (e.g. up to 6.6 dB in SER for non-piecewise constant neuroimage)
- Not restricted to coil geometry
- W/o having more serious inhomogeneity artifacts caused by smaller diameter receive coils, it can achieve a better CS recovery guarantee (decreasing the value of s_c 's).

Recovery Guarantee and Coil Geometry Design

- Suggestions³⁸
 - ▶ Smaller diameter coils to reduce s_c for $c = 1, \dots, C$
 - ▶ An increase of the inter-element gap between coils
 - ▶ A larger number of coils while avoiding redundancy

³⁸P. B. Roemer, W. A. Edelstein, C. E. Hayes, *et al.*, "The NMR phased array", *Magn. Reson. Med.*, vol. 16, no. 2, pp. 192–225, 1990, J. A. de Zwart, P. J. Ledden, P. Kellman, *et al.*, "Design of a SENSE-optimized high-sensitivity MRI receive coil for brain imaging", *Magn. Reson. Med.*, vol. 47, no. 6, pp. 1218–1227, 2002.

Outline

1 CS and Parallel Acquisition

- Introduction
- Abstract Framework and Main Theorem
- Main Results: Distinct Sampling
- Main Results: Identical Sampling
- Numerical Experiments
- Conclusions

2 JS CS SENSE pMRI

- Introduction
- Theory & Methods
- Results & Discussion
- Conclusions

3 Future Research

4 Appx.

- CS and Parallel Acquisition
- JS CS SENSE pMRI

5 Appx.: CS X-Ray CT

Future Research

Theoretical CS (collab: Prof. Adcock)

- Probabilistic sensor profile models in CS parallel acquisition system
- Practical CS using prior information
- Non-uniform FFT in CS

CS in Computational Imaging

- Combination with machine learning (ML)
- CS-based encoding in parallel transmit & receive SENSE MRI¹
- CS-based encoding in X-ray CT²

Image Analysis in Neuroimaging

- Randomized paired difference analysis with complete & incomplete pairs³ (collab: S. Bari)
- ML for brain injury detection (collab: J. Jin, I. Jang, Dr. K. Han, and Dr. M. Kwon)

¹K. Pawar, G. Egan, and J. Zhang, "Multichannel compressive sensing MRI using noiselet encoding", *PLoS ONE*, vol. 10, no. 5, e0126386, 2015.

²W. Hou and C. Zhang, "Analysis of compressed sensing based CT reconstruction with low radiation", in *Proc. 2014 Intell. Signal Process. Commun. Syst.*, Sarawak, Malaysia, 2014, pp. 291–296.

³S. Bari, I. Y. Chun, L. J. Leverenz, *et al.*, "DTI detection of WM abnormalities using randomization test with complete and incomplete pairs", in *Proc. 21st Org. for Hum. Brain Mapp.*, Honolulu, HI, 2015.

Acknowledgements

- I would like to thank to Prof. Adcock and Prof. Talavage.
- I appreciate the financial support from DMS of National Science Foundation (NSF) and Indiana State Department of Health (ISDH) that funded parts of the research discussed in this presentation.
- I would like to thank Prof. Fessler for his kind invitation.

Q & A

Thank you for your attention.

Continue?

Outline

1 CS and Parallel Acquisition

- Introduction
- Abstract Framework and Main Theorem
- Main Results: Distinct Sampling
- Main Results: Identical Sampling
- Numerical Experiments
- Conclusions

2 JS CS SENSE pMRI

- Introduction
- Theory & Methods
- Results & Discussion
- Conclusions

3 Future Research

4 Appx.

- CS and Parallel Acquisition
- JS CS SENSE pMRI

5 Appx.: CS X-Ray CT

Framework: Distinct Sampling

- Recall:

- ▶ $D = 1$ and $p = m = \sum_{c=1}^C m_c$
- ▶ $\mathbf{A}: \mathbf{A}_c \in \mathbb{C}^{m_c \times N}$ drawn from possibly distinct distributions

- F_1, \dots, F_C are jointly isotropic:

$$\sum_{c=1}^C \frac{m_c}{m} \mathbb{E}(\mathbf{a}_c \mathbf{a}_c^*) = \mathbf{I}, \quad \mathbf{a}_c \sim F_c, \quad c = 1, \dots, C. \quad (7)$$

- ▶ F_c : distribution on \mathbb{C}^N for $c = 1, \dots, C$

- Define the new distribution F on \mathbb{C}^N :

Conditioned on the event $\{X = c\}$, $F = F_c$.

- ▶ $\mathbb{P}(X = c) = m_c/m$ for $c = 1, \dots, C$
- ▶ If $\mathbf{a} \in \mathbb{C}^N$ denotes an arbitrary row of \mathbf{A} , then \mathbf{a} arises from the distribution F_c with probability m_c/m .

-

$$\mathbf{A} = \frac{1}{\sqrt{m}} \begin{bmatrix} \mathbf{A}_1 \\ \vdots \\ \mathbf{A}_C \end{bmatrix} \in \mathbb{C}^{m \times N}$$

- ▶ $\mathbf{A}_c \in \mathbb{C}^{q_c \times N}$: contains the rows of \mathbf{A} drawn from F_c
- ▶ q_c : the number of such rows drawn from F_c ; $\mathbb{E}(q_c) = m_c$

Framework: Distinct Sampling

Sensor profile matrices $\mathbf{H}_c \neq \mathbf{I}$

- $\mathbf{A}_c = \tilde{\mathbf{A}}_c \mathbf{H}_c$
 - ▶ $\tilde{\mathbf{A}}_c \in \mathbb{C}^{m/C \times N}$: CS matrix drawn from (possibly different) isotropic distribution G_c on \mathbb{C}^N
 - ▶ $\mathbf{H}_c \in \mathbb{C}^{N \times N}$: sensor profile matrices (e.g. $\text{diag}(\mathbf{h}_c)$ and $\text{circ}(\mathbf{h}_c)$)
 - ▶ $\mathbf{a}_c \sim F_c$ if $\mathbf{a}_c = \mathbf{H}_c^* \tilde{\mathbf{a}}_c$ for $\tilde{\mathbf{a}}_c \sim G_c$.
- Joint isometry condition from (7):

$$\frac{1}{C} \sum_{c=1}^C \mathbf{H}_c^* \mathbf{H}_c = \mathbf{I}$$

- Incoherent G_c 's:

$$\mu_G = \max_{c=1, \dots, C} \mu(G_c)$$

Framework: Identical Sampling

- Recall:

- ▶ $D = C$ and $p = m/C$

- ▶ \mathbf{A} : $\mathbf{A}_c = \tilde{\mathbf{A}}\mathbf{H}_c$, $\tilde{\mathbf{A}} \in \mathbb{C}^{m/C \times R}$: random; $\mathbf{H}_c \in \mathbb{C}^{R \times N}$: fixed & deterministic

- ▶ $\tilde{\mathbf{A}} = \frac{1}{p} \sum_{i=1}^p \mathbf{e}_i \mathbf{a}_i^*$

- ▶ $\mathbf{a}_i \sim G$, where G is isotropic on \mathbb{C}^R

- Define the distribution F on the space of $R \times C$ complex matrices:

$$\mathbf{B} = [\mathbf{H}_1^* \mathbf{a} \mid \cdots \mid \mathbf{H}_C^* \mathbf{a}] \sim F$$

- ▶ $\mathbf{a} \sim G$

- Joint isometry condition: Isotropic F in the sense of (2)

$$\sum_{c=1}^C \mathbf{H}_c^* \mathbf{H}_c = \mathbf{I}$$

Sparsity Models: Sparsity in Levels

Definition 3 (Sparsity in levels¹)

Let $\mathcal{I} = \{I_1, \dots, I_C\}$ be a partition of $\{1, \dots, N\}$ and $\mathcal{S} = (s_1, \dots, s_C) \in \mathbb{N}^C$ where $s_c \leq |I_c|$ for $c = 1, \dots, C$. We say that $\mathbf{z} \in \mathbb{C}^N$ is $(\mathcal{S}, \mathcal{I})$ -sparse in levels if

$$|\{j : z_j \neq 0\} \cap I_c| \leq s_c, \quad c = 1, \dots, C.$$

We denote the set of such vectors as $\Sigma_{\mathcal{S}, \mathcal{I}}$ and, for an arbitrary $\mathbf{x} \in \mathbb{C}^N$, write

$$\sigma_{\mathcal{S}, \mathcal{I}}(\mathbf{x})_1 = \min \{\|\mathbf{x} - \mathbf{z}\|_1 : \mathbf{z} \in \Sigma_{\mathcal{S}, \mathcal{I}}\},$$

for the error of the best ℓ^1 -norm approximation of \mathbf{x} by an $(\mathcal{S}, \mathcal{I})$ -sparse vector.

- Approximation in $\Sigma_{\mathcal{S}, \mathcal{I}}$ means approximation by the largest s_c absolute entries of \mathbf{x} restricted to I_c for $c = 1, \dots, C$.

¹I. Y. Chun and B. Adcock, "Compressed sensing and parallel acquisition", *Submitted to IEEE Trans. Inf. Theory*, 2016. [Online]. Available: <http://arxiv.org/abs/1601.06214>, B. Adcock, A. C. Hansen, C. Poon, et al., "Breaking the coherence barrier: A new theory for compressed sensing", *ArXiv pre-print cs.IT/1302.0561*, 2013

Refined Coherence

Definition 4 (Coherence relative to Δ)

Let F be a distribution on the space of $N \times D$ complex matrices and $\Delta \subseteq \{1, \dots, N\}$. We define the local coherence of F relative to Δ as

$$\Gamma(F, \Delta) = \max \{ \Gamma_1(F, \Delta), \Gamma_2(F, \Delta) \},$$

where $\Gamma_1(F, \Delta)$ and $\Gamma_2(F, \Delta)$ are the smallest quantities such that

$$\|\mathbf{B}\mathbf{B}^*\mathbf{P}_\Delta\|_\infty \leq \Gamma_1(F, \Delta), \quad \mathbf{B} \sim F,$$

and

$$\sup_{\substack{z \in \mathbb{C}^N \\ \|z\|_\infty = 1}} \max_{i=1, \dots, N} \mathbb{E} |e_i^* \mathbf{B}\mathbf{B}^* \mathbf{P}_\Delta z|^2 \leq \Gamma_2(F, \Delta), \quad \mathbf{B} \sim F,$$

almost surely. Note that $\Gamma_i(F, \Delta) \geq 1$, $i = 1, 2$, due to the isotropic assumption on F .

- **Note:** The definition of local coherence in levels is omitted in this talk.

¹ F is isotropic in the sense that $\mathbb{E}(\mathbf{B}\mathbf{B}^*) = \mathbf{I}$, $\mathbf{B} \sim F$.

Ideas behind the proof of Theorem 2

- ① Lemma 5: Recovery is guaranteed by the existence of a so-called dual certificate (ρ)
- ② Golfing scheme of Gross²: Find a suitable dual certificate

Lemma 5

Let $\mathbf{A} \in \mathbb{C}^{m \times N}$, where $m \leq N$, and $\Delta \subseteq \{1, \dots, N\}$. Suppose that

$$(i) : \|\mathbf{P}_\Delta \mathbf{A}^* \mathbf{A} \mathbf{P}_\Delta - \mathbf{P}_\Delta\|_2 \leq \alpha, \quad (ii) : \max_{i \notin \Delta} \{\|\mathbf{P}_\Delta \mathbf{A}^* \mathbf{A} \mathbf{e}_i\|_2\} \leq \beta,$$

and that there exists a vector $\rho = \mathbf{A}^* \xi \in \mathbb{C}^m$ for some $\xi \in \mathbb{C}^m$ such that

$$(iii) : \|\mathbf{P}_\Delta \rho - \text{sign}(\mathbf{P}_\Delta \mathbf{x})\|_2 \leq \gamma, \quad (iv) : \|\mathbf{P}_\Delta^\perp \rho\|_\infty \leq \theta, \quad (v) : \|\xi\| \leq \sigma \sqrt{|\Delta|},$$

for constants $0 \leq \alpha < 1$ and $\beta, \gamma, \theta, \sigma \geq 0$ satisfying $\theta + \beta\gamma/(1 - \alpha) < 1$. For a vector $\mathbf{x} \in \mathbb{C}^N$, $\text{sign}(\mathbf{x}) \in \mathbb{C}^N$ denotes its complex sign. Let $\mathbf{x} \in \mathbb{C}^N$, $\mathbf{y} = \mathbf{A}\mathbf{x} + \mathbf{e}$ with $\|\mathbf{e}\|_2 \leq \eta$ and suppose that $\hat{\mathbf{x}}$ is a minimizer of the problem

$$\min_{\mathbf{z} \in \mathbb{C}^N} \|\mathbf{z}\|_1 \text{ subject to } \|\mathbf{A}\mathbf{z} - \mathbf{y}\|_2 \leq \eta.$$

Then the estimate

$$\|\hat{\mathbf{x}} - \mathbf{x}\|_2 \leq C_1 \|\mathbf{x} - \mathbf{P}_\Delta \mathbf{x}\|_1 + C_2 \left(1 + \sigma \sqrt{|\Delta|}\right) \eta,$$

holds for constants C_1 and C_2 depending on α , β , γ and θ only.

²D. Gross, "Recovering low-rank matrices from few coefficients in any basis", *IEEE Trans. Inform. Theory*, vol. 57, no. 3, pp. 1548–1566, 2011.

Main Results: Distinct Sampling

Corollary 6 (Distinct sampl. with sparsity model³)

Consider the distribution F defined in slide 48 and suppose that $\mathbf{x} \in \mathbb{C}^N$, $0 < \epsilon < 1$ and $N \geq s \geq 2$. Draw $\mathbf{A} \in \mathbb{C}^{m \times N}$ according to (1) and let $\mathbf{y} = \mathbf{A}\mathbf{x} + \mathbf{e}$ with $\|\mathbf{e}\|_2 \leq \eta$. Then for any minimizer $\hat{\mathbf{x}}$ of

$$\min_{\mathbf{z} \in \mathbb{C}^N} \|\mathbf{z}\|_1 \text{ subject to } \|\mathbf{A}\mathbf{z} - \mathbf{y}\|_2 \leq \eta,$$

we have

$$\|\mathbf{x} - \hat{\mathbf{x}}\|_2 \lesssim \sigma_s(\mathbf{x})_1 + \sqrt{s}\eta,$$

with probability at least $1 - \epsilon$, provided

$$m \gtrsim s \cdot \left(\max_{c=1, \dots, C} \mu(F_c) \right) \cdot L,$$

where μ is a standard coherence, F_1, \dots, F_C are as in slide 48 and L is as in (5).

³I. Y. Chun and B. Adcock, "Compressed sensing and parallel acquisition", *Submitted to IEEE Trans. Inf. Theory*, 2016. [Online]. Available: <http://arxiv.org/abs/1601.06214>

Main Results: Distinct Sampling

Corollary 7 (Distinct sampl. with sparsity model and diag. profiles⁴)

Let $\mathbf{x} \in \mathbb{C}^N$, $0 < \epsilon < 1$, $N \geq s \geq 2$ and suppose that $\mathbf{H}_c \in \mathbb{C}^{N \times N}$, $c = 1, \dots, C$, are diagonal matrices satisfying the joint isometry condition, i.e. $C^{-1} \sum_{c=1}^C \mathbf{H}_c^* \mathbf{H}_c = \mathbf{I}$. Let G_1, \dots, G_C be isotropic distributions on \mathbb{C}^N and for $c = 1, \dots, C$ define F_c so that $\mathbf{a}_c \sim F_c$ if $\mathbf{a}_c = \mathbf{H}_c^* \tilde{\mathbf{a}}_c$ for $\tilde{\mathbf{a}}_c \sim G_c$. Let F be as in slide 48 for this choice of F_1, \dots, F_C and set $m_1 = \dots = m_C = m/C$. Draw \mathbf{A} according to (1) and let $\mathbf{y} = \mathbf{A}\mathbf{x} + \mathbf{e}$ with $\|\mathbf{e}\|_2 \leq \eta$. Then for any minimizer $\hat{\mathbf{x}}$ of

$$\min_{\mathbf{z} \in \mathbb{C}^N} \|\mathbf{z}\|_1 \text{ subject to } \|\mathbf{A}\mathbf{z} - \mathbf{y}\|_2 \leq \eta,$$

we have

$$\|\mathbf{x} - \hat{\mathbf{x}}\|_2 \lesssim \sigma_s(\mathbf{x})_1 + \sqrt{s}\eta,$$

with probability at least $1 - \epsilon$, provided

$$m \gtrsim s \cdot \mu_G \cdot \left(\max_{c=1, \dots, C} \|\mathbf{H}_c\|_\infty^2 \right) \cdot L,$$

where $\mu_G = \max_{c=1, \dots, C} \mu(G_c)$ and L is as in (5).

⁴I. Y. Chun and B. Adcock, "Compressed sensing and parallel acquisition", *Submitted to IEEE Trans. Inf. Theory*, 2016. [Online]. Available: <http://arxiv.org/abs/1601.06214>

Diagonal Sensor Profile Matrix

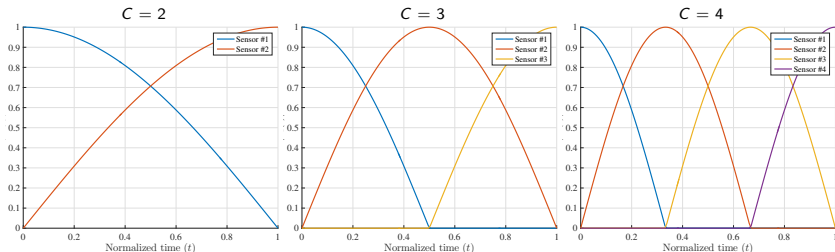


Figure: Magnitudes of diagonal sensor profiles ($C = 2, 3, 4$)⁵

⁵I. Y. Chun and B. Adcock, "Compressed sensing and parallel acquisition", *Submitted to IEEE Trans. Inf. Theory*, 2016. [Online]. Available: <http://arxiv.org/abs/1601.06214>.

CS SENSE pMRI Reconstruction

Theorem 8 (Nonuniform recovery in CS SENSE⁶)

Assume that $\mathbf{U} = [(\Phi \text{diag}(\mathbf{h}_1)\Psi)^* | \dots | (\Phi \text{diag}(\mathbf{h}_C)\Psi)^*]^*$ where $\Psi = \mathbf{I}$, and $\sum_c |\text{diag}(\mathbf{h}_c)|^2 = \mathbf{I}$. Let $\Delta \subseteq \{1, \dots, N\}$, $|\Delta| = s$ be given. For $0 < \epsilon < 1$, if

$$m \gtrsim \eta \rho^{-2} C s \log(\epsilon^{-1}) \log(N),$$

then, for $\rho \in (0, 1)$, the normalized matrix $\tilde{\mathbf{A}}_\Delta = (1/\sqrt{m})\mathbf{P}_\Omega \mathbf{U}$ satisfies

$$\|\tilde{\mathbf{A}}_\Delta^* \tilde{\mathbf{A}}_\Delta - \mathbf{I}\|_{2 \rightarrow 2} \leq \rho$$

with probability at least $1 - \epsilon$, where $\|\mathbf{A}\|_{2 \rightarrow 2} := \max_{\|\mathbf{x}\|_2=1} \|\mathbf{A}\mathbf{x}\|_2$.[†]

- Note that the condition on $\|\tilde{\mathbf{A}}_\Delta^* \tilde{\mathbf{A}}_\Delta - \mathbf{I}\|_{2 \rightarrow 2}$ is **necessary**, but not sufficient, to ensure a stable and robust CS signal recovery.

⁶I. Y. Chun, B. Adcock, and T. M. Talavage, "Efficient compressed sensing SENSE pMRI reconstruction with joint sparsity promotion", *IEEE Trans. Med. Imag.*, vol. 35, no. 1, pp. 354–368, 2016

Efficient $\|\cdot\|_{2,1}$ -Norm Minimization by SB and VS¹⁰

By **simplified Bregman iteration**, (6) can be reduced to a sequence of unconstrained problems:

$$\mathbf{x}^{(k+1)} = \underset{\mathbf{x}^{(k)}}{\operatorname{argmin}} \|\Psi_{\mathbf{C}}\mathbf{H}\mathbf{x}^{(k)}\|_{2,1} + (\alpha/2)\|\mathbf{y}^{(k)} - \mathbf{F}_{\bar{\Omega}}\mathbf{H}\mathbf{x}^{(k)}\|_2^2; \quad \mathbf{y}^{(k+1)} = \mathbf{y}^{(k)} + \mathbf{y} - \mathbf{F}_{\bar{\Omega}}\mathbf{H}\mathbf{x}^{(k+1)}.$$

By **variable splitting** (VS⁸, $\mathbf{d}_{\mathbf{H}}^{(k)} = \mathbf{H}\mathbf{x}^{(k)}$, separating an effect of \mathbf{H} on $\mathbf{d}_{\Psi}^{(k)} = \Psi_{\mathbf{C}}\mathbf{H}\mathbf{x}^{(k)}$) and **split Bregman** (SB⁹, $\mathbf{d}_{\Psi}^{(k)} = \Psi_{\mathbf{C}}\mathbf{d}_{\mathbf{H}}^{(k)}$) method,

$$\begin{aligned} (\mathbf{x}^{(k+1)}, \mathbf{d}_{\mathbf{H}}^{(k+1)}, \mathbf{d}_{\Psi}^{(k+1)}) = \underset{\mathbf{x}^{(k)}, \mathbf{d}_{\mathbf{H}}^{(k)}, \mathbf{d}_{\Psi}^{(k)}}{\operatorname{argmin}} & \|\mathbf{d}_{\Psi}^{(k)}\|_{2,1} + (\alpha/2)\|\mathbf{y}^{(k)} - \mathbf{F}_{\bar{\Omega}}\mathbf{d}_{\mathbf{H}}^{(k)}\|_2^2 + \\ & (\nu/2)\|\mathbf{d}_{\mathbf{H}}^{(k)} - \mathbf{H}\mathbf{x}^{(k)} - \mathbf{b}_{\mathbf{H}}^{(k)}\|_2^2 + (\beta/2)\|\mathbf{d}_{\Psi}^{(k)} - \Psi_{\mathbf{C}}\mathbf{d}_{\mathbf{H}}^{(k)} - \mathbf{b}_{\Psi}^{(k)}\|_2^2; \\ \mathbf{b}_{\mathbf{H}}^{(k+1)} = \mathbf{b}_{\mathbf{H}}^{(k)} + \mathbf{H}\mathbf{x}^{(k+1)} - \mathbf{d}_{\mathbf{H}}^{(k+1)}; & \quad \mathbf{b}_{\Psi}^{(k+1)} = \mathbf{b}_{\Psi}^{(k)} + \Psi_{\mathbf{C}}\mathbf{d}_{\mathbf{H}}^{(k+1)} - \mathbf{d}_{\Psi}^{(k+1)}. \end{aligned}$$

Decomposed l_1 and l_2 components \rightarrow Efficient solution!

⁷ **“Adding back the noise”**: Regularization parameter plays important role only in convergence rate, but does not affect on the solution by varying observation.

⁸S. Ramani and J. A. Fessler, “A splitting-based iterative algorithm for accelerated statistical X-ray CT reconstruction”, *IEEE Trans. Med. Imag.*, vol. 31, no. 3, pp. 677–688, 2012.

⁹T. Goldstein and S. Osher, “The split Bregman method for L1-regularized problems”, *SIAM J. Imaging Sci.*, vol. 2, no. 2, pp. 323–343, 2009.

¹⁰I. Y. Chun, B. Adcock, and T. M. Talavage, “Efficient compressed sensing SENSE pMRI reconstruction with joint sparsity promotion”, *IEEE Trans. Med. Imag.*, vol. 35, no. 1, pp. 354–368, 2016.

CaL JS CS SENSE pMRI Reconstruction

Basic Framework of Sensitivity Estimation w/o Calib. Scanning

- ① Simultaneous acquisition of k -space data for multiple surface-coils and single body-coil
- ② Reconstruction of multiple surface-coil images (\mathbf{x}_C^*) and a single body-coil image (\mathbf{x}_0^*)
- ③ Sensitivity estimation using \mathbf{x}_C^* and \mathbf{x}_0^*

Residual-JS Regularized Sensitivity Estimation¹¹

$$\underset{\mathbf{r}}{\operatorname{argmin}} \left\| \Psi_C(\mathbf{x}_C^* - \underbrace{\begin{bmatrix} \operatorname{dg}(\mathbf{x}_0^*)\mathbf{R} & & \\ & \ddots & \\ & & \operatorname{dg}(\mathbf{x}_0^*)\mathbf{R} \end{bmatrix}}_{=: \mathbf{X}} \underbrace{\begin{bmatrix} \mathbf{r}_1 \\ \vdots \\ \mathbf{r}_C \end{bmatrix}}_{=: \mathbf{r}} \right\|_{2,1} \quad \text{s.t. } \|\mathbf{x}_C^* - \mathbf{X}\mathbf{r}\|_2^2 < \delta$$

- ▶ $\mathbf{r} \in \mathbb{C}^{PC}$, in which $\mathbf{r}_c \in \mathbb{C}^P$: the c^{th} coil coefficient vector; $\mathbf{X} \in \mathbb{C}^{NC \times PC}$
- ▶ $\mathbf{R} \in \mathbb{C}^{N \times P}$: mapping matrix of the coeff. (of complex sinusoid basis functions¹²) to data

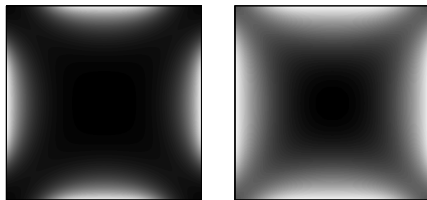
Calibration-Less (CaL) JS CS SENSE

¹¹I. Y. Chun, B. Adcock, and T. M. Talavage, "Efficient compressed sensing SENSE pMRI reconstruction with joint sparsity promotion", *IEEE Trans. Med. Imag.*, vol. 35, no. 1, pp. 354–368, 2016.

¹²M. Guerquin-Kern, L. Lejeune, K. P. Pruessmann, *et al.*, "Realistic analytical phantoms for parallel Magnetic Resonance Imaging", *IEEE Trans. Med. Imag.*, vol. 31, no. 3, pp. 626–636, 2012.

Simulation Setup II

- Tested image: T_1 -weighted brain image with size of 512×512
- Sensitivity map simulation with a **larger-sized coil** setup (for state-of-the-art methods): $C = 4$; a coil radius of 9 cm; a distance from the coil centers to the center of the rectangular FOV of 18 cm
→ avoidance of serious inhomogeneity artifacts in the SoS-combined image
- Body-coil k -space data: sampled along the same radial trajectories; strong noise (20 dB SNR) for realization of complex Gaussian noise
- CaL SENSE-based CS reconstruction
 - ▶ Body-coil image (\mathbf{x}_0^*) recon. parameters: 4-level Symlet with 4 vanishing moments, total variation (TV); 5×100 iterations
 - ▶ \mathbf{x}_C^* by coil-by-coil recon: DDT-4, TV (CaLM_{W+TV})
 - ▶ Residual-JS regularized sensitivity est.: DDT-4, $\text{supp}(\text{SoS}(\mathbf{x}_C^*))$ -based estimation



Coil-setup I

Coil-setup II of larger coils

Figure: An example of SoS of sensitivity profiles ($C = 4$)

CaL JS CS SENSE vs State-of-the-Art Methods

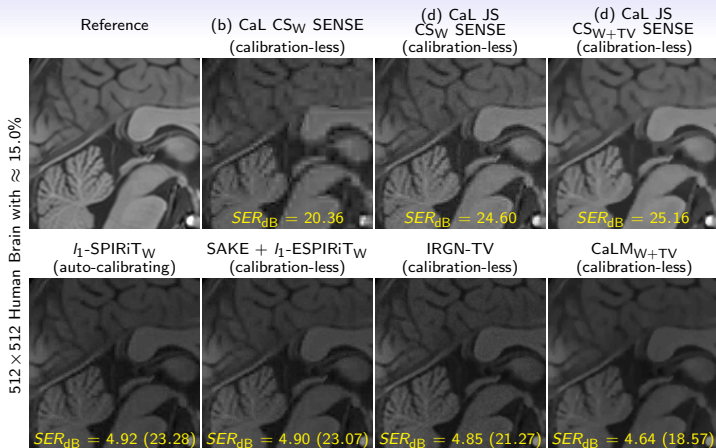
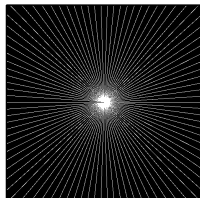


Figure: Comparison of 512 × 512 reconstructed images from different auto-calibrating or calibration-less pMRI reconstruction models (≈ 15.0% noisy measurements and $C = 4$): (b), (c), and (d) are calibration-less reconstruction based on the residual-JS regularized sensitivity estimation. CaL JS CS SENSE outperforms other state-of-the-art calibration-less reconstruction methods for the non-piecewise constant image: the SER gap is in the interval [1.9, 6.6] dB.¹⁴

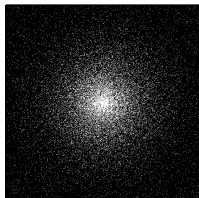
¹⁴The SER_{dB} in parenthesis is defined by $SER_{dB}(k) = 20 \log_{10}(\|\text{SoS}(\mathbf{x}_C^{true})\|_2 / \|\text{SoS}(\mathbf{x}_C^{true}) - \text{SoS}(\mathbf{x}_C^{(k)})\|_2)$.

Nonuniform Density Random Sampling

- Nonuniform density random sampling is necessary to overcome the MC barrier in CS: e.g. **multi-level random sampling**¹⁵
- Nonuniform under-sampling along the phase-encoding direction: Worse recovery guarantee than multi-level scheme¹⁶
- **Radial line sampling**: Sufficiently close to the optimal multi-level sampling, i.e. $\lesssim 1.5$ dB in signal-to-error ratio (SER) for GLPU phantom image reconstruction¹⁷



Radial line



Multi-level

Figure: Sampling schemes (sampling ratio ≈ 10 %)

¹⁵B. Adcock, A. C. Hansen, C. Poon, *et al.*, "Breaking the coherence barrier: A new theory for compressed sensing", *ArXiv pre-print cs.IT/1302.0561*, 2013.

¹⁶J. Bigot, C. Boyer, and P. Weiss, "An analysis of block sampling strategies in compressed sensing", *ArXiv preprint cs.IT:1305.4446*, 2013.

¹⁷I. Y. Chun, B. Adcock, and T. Talavage, "Efficient compressed sensing SENSE parallel MRI reconstruction with joint sparsity promotion and mutual incoherence enhancement", in *Proc. 36th IEEE EMBS, Chicago, IL, 2014*, pp. 2424–2427.

Summary of Recovery Guarantee

- (a) case: $m \gtrsim \eta s \log(N)$ for all three models
- (b) case: Recovery guarantee for JS CS SENSE is better than CS SENSE and similar to the coil-by-coil CS model.
However, due to error propagation lemma, reconstruction error of JS CS SENSE is expected to be smaller than (SoS-based) coil-by-coil CS.
- JS CS SENSE vs CS SENSE: $\sum_c s_c$ (or $\max_c s_c$) vs sC ;
Greater difference in low-resolution imaging

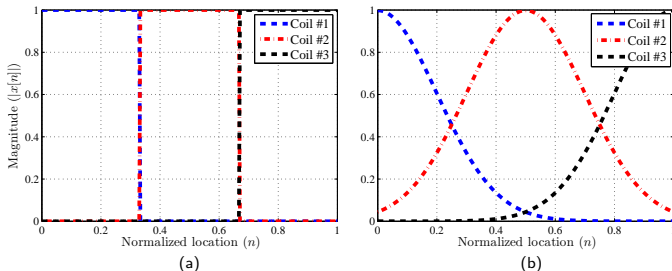


Figure: An example of shape of coil sensitivity profiles in 1D ($C = 3$): (a) perfect partitioning and (b) realistic case

Outline

1 CS and Parallel Acquisition

- Introduction
- Abstract Framework and Main Theorem
- Main Results: Distinct Sampling
- Main Results: Identical Sampling
- Numerical Experiments
- Conclusions

2 JS CS SENSE pMRI

- Introduction
- Theory & Methods
- Results & Discussion
- Conclusions

3 Future Research

4 Appx.

- CS and Parallel Acquisition
- JS CS SENSE pMRI

5 Appx.: CS X-Ray CT

Background

- Minimization problem for non-convex CS

$$\operatorname{argmin}_{\mathbf{x}} \|\Psi \mathbf{x}\|_p^p, \quad \text{s.t. } \mathbf{y} = \mathbf{P}_\Omega \Phi \mathbf{x},$$

with l_p ($p \in (0, 1)$)-quasi-norm, defined by $\|\mathbf{x}\|_p^p = \sum_{n=1}^N |x_n|^p$.

- Perfect recovery of s -sparse solution of $\mathbf{y} = \mathbf{P}_\Omega \Phi \mathbf{x}$ with high probability, if Φ has i.i.d. Gaussian entries and $\Psi = \mathbf{I}$ ¹⁸
- Recovery guarantee

$$M \geq C_1(p)s + pC_2(p)s \log(N/s),$$

where the constants $C_1(p)$ and $C_2(p)$ decrease as $p \rightarrow 0$.

- NP-hard problem
Local minimum, if $\Psi \mathbf{x}$ decays quickly and m is sufficiently large¹⁹.

¹⁸R. Chartrand and V. Staneva, "Restricted isometry properties and nonconvex compressive sensing", *Inverse Probl.*, vol. 24, no. 3, p. 035 020, 2008, Y. Shen and S. Li, "Restricted p -isometry property and its application for nonconvex compressive sensing", *Adv. Comput. Math.*, vol. 37, no. 3, pp. 441–452, 2012.

¹⁹D. Ge, X. Jiang, and Y. Ye, "A note on complexity of L_p minimization", *Math. Program.*, vol. 129, no. 2, pp. 285–299, 2011.

T-DFST & Non-Convex CS

Tensor Discrete Fourier Slice Theorem (T-DFST)²⁰

- Exact mapping of 1D discrete Fourier transform (DFT) of discrete Radon transform (DRT) data on a Cartesian 2D DFT grid
: Avoidance of **interpolation errors**
- Relates CS theory with line-based projection sampling system.

Non-Convex CS

- Uniform random sampling of projection angles + T-DFST
= **nonuniform random Fourier measurement** on the 2D Cartesian grid
- Reduction of sufficient number of measurements by enhancing sparsity
- Solved by efficient constrained reweighted l_1 -norm minimization based on split Bregman (SB) and majorization-minimization (MM)

²⁰I. Y. Chun, B. Adcock, and T. Talavage, "Non-convex compressed sensing CT reconstruction based on tensor discrete fourier slice theorem", in *Proc. 36th IEEE EMBS*, Chicago, IL, 2014, pp. 5141–5144.

T-DFST- & CS-based Reconstructed Images

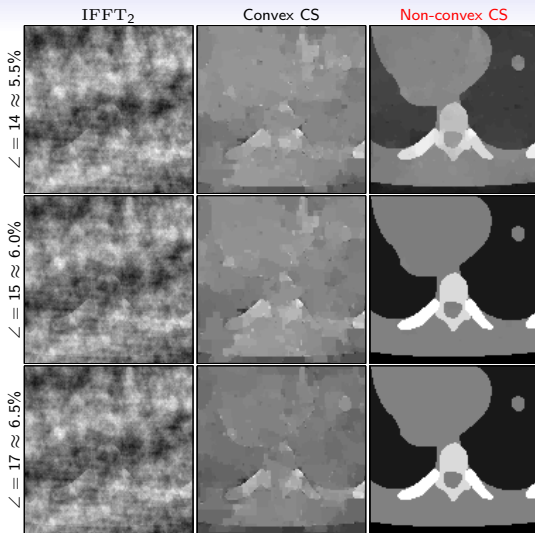


Figure: Comparison of reconstructed 257×257 NCAT phantom images from different CT reconstruction methods and angles. Y. Chun, B. Adcock, and T. Talavage, "Non-convex compressed sensing CT reconstruction based on tensor discrete fourier slice theorem", in *Proc. 36th IEEE EMBS, Chicago, IL, 2014*, pp. 5141–5144

Optimality and Practical Applicability of T-DFST

Optimality of nonuniform random sampling of Fourier samples based on T-DFST, by uniformly random sampling projection angles

- **Only suboptimal:** Periodicity assumption and modulation operator lead to run against a mutual coherence (MC) barrier.

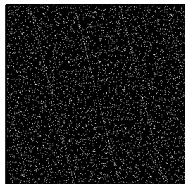


Figure: Partial 2D DFT by uniform sampling of 17 angles at random for $N = 257^{21}$

Practical applicability of T-DFST

- Difficulty to implement nonuniform ray spacing with different angles in DRT
- How close is DRT-based proj. model to a line-based continuous Radon transform model?

²¹I. Y. Chun, B. Adcock, and T. Talavage, "Non-convex compressed sensing CT reconstruction based on tensor discrete fourier slice theorem", in *Proc. 36th IEEE EMBS, Chicago, IL, 2014*, pp. 5141–5144.